Original Article

The clinical value of spectral computed tomography reconstruction technology for the anatomy of the superior mesenteric artery in laparoscopic radical right hemicolectomy for colon cancer: a cross-sectional study

Jinghao Chen, Hao Tian, Ke Yu, Shumin Tao, Bin Bai, Anyi Song, Hongmei Gu

Department of Medical Imaging, Affiliated Hospital of Nantong University, Nantong, China

Contributions: (I) Conception and design: J Chen; (II) Administrative support: H Gu; (III) Provision of study materials or patients: H Gu, H Tian; (IV) Collection and assembly of data: J Chen, K Yu, B Bai; (V) Data analysis and interpretation: S Tao, A Song; (VI) Manuscript writing: All authors; (VII) Final approval of manuscript: All authors.

Correspondence to: Hongmei Gu, MD. Department of Medical Imaging, Affiliated Hospital of Nantong University, No. 20 Xisi Road, Chongchuan District, Nantong 226001, China. Email: guhongmei71@163.com.

Background: The superior mesenteric artery (SMA) has numerous branches and a high rate of anatomical variation, making it challenging to manage during surgery. This study aimed to evaluate the clinical utility of dual energy computed tomography (CT) three-dimensional (3D) reconstruction combined with arteriovenous image fusion technology for assessing SMA variations. The goal is to aid in surgical planning for laparoscopic radical resection of right colon cancer, using the SMA as the primary surgical approach.

Methods: We performed a retrospective analysis of clinical and imaging data from patients with right colon cancer who underwent enhanced spectral CT of the abdomen and pelvis before surgery at Affiliated Hospital of Nantong University from January 2020 to June 2024. Using post-processing techniques to reconstruct SMA images, the study evaluated the SMA root position, measured the distance between the roots of the right branches of the SMA, analyzed their relationship with patient gender and body mass index (BMI), and summarized the types of right branches of the SMA. Additionally, the relationship between the middle colic artery (MCA), right colic artery (RCA), ileocolic artery (ICA), and the superior mesenteric vein (SMV) positions were analyzed in relation to patient clinical characteristics.

Results: The SMA root was mostly located at the L1 vertebral level (74.68%, 236/316), with a vertebral range between T12–L2. The distance from the SMA root to the abdominal aorta (D_{SMA-AB}) was 115.97±11.82 mm, and this distance increased with higher BMI in males. Type I SMA (presence of RCA) accounted for 39.87% (126/316), Type II (absence of RCA) accounted for 60.13% (190/316), with the distance between the root of the MCA and the ICA ($d_{MCA-ICA}$) being longer in type II. 91.27% (115/126) of the RCA was anterior to the SMV. When the RCA was posterior, the ICA was always posterior to the SMV. The ICA was anterior to the SMV in about 50.63% (160/316) of cases, with a higher incidence in males and those with a shorter $d_{MCA-ICA}$.

Conclusions: Spectral CT 3D reconstruction and arteriovenous image fusion technology can accurately assess the anatomical features of the SMA and the relationship between the right branch vessels and the SMV, helping to develop reasonable surgical plans for laparoscopic radical right hemicolectomy in patients with right colon cancer using an "SMA-prioritized approach".

Keywords: Superior mesenteric artery (SMA); middle colic artery (MCA); ileocolic artery (ICA); three-dimensional reconstruction (3D reconstruction)

Submitted Mar 05, 2025. Accepted for publication May 08, 2025. Published online Aug 22, 2025. This article was updated on Oct 28, 2025.

The original version was available at: https://dx.doi.org/10.21037/jgo-2025-167

doi: 10.21037/jgo-2025-167

Introduction

The superior mesenteric artery (SMA) is the main blood supply vessel for the third and fourth part of the duodenum, jejunum, ileum, cecum, appendix, ascending colon, and the right two-thirds of the transverse colon (1). Lesions within the SMA lumen, such as embolism or thrombosis, and morphological changes in the vessel wall, such as dissection, aneurysm, mural thrombus, intramural hematoma, and atherosclerotic plaque, can lead to abnormal blood flow, causing intestinal ischemia and potentially leading to irreversible serious symptoms like bowel necrosis (2,3). Anatomical variations of the SMA, including branching patterns, pathways, and relationships with the and the superior mesenteric vein (SMV), also affect the surgical resection of substantial or hollow organs involving the SMA in the abdomen (4,5).

Laparoscopic radical right hemicolectomy for right colon cancer (involving the cecum, ascending colon, hepatic flexure, and right third of the transverse colon) requires a high level of preoperative understanding of SMA anatomical variations. This is due to the narrow field of view and the loss of tactile feedback during laparoscopic surgery, making it challenging to judge vascular branch variations intraoperatively (6,7). Additionally, the principles of complete mesocolic excision (CME) and maximizing lymph node clearance currently emphasize an "SMA-prioritized approach" for laparoscopic radical right hemicolectomy, necessitating a more precise preoperative assessment of SMA anatomical variations (8-13). Identifying the positions of the ileocolic artery (ICA) roots can quickly help clinicians locate key structures (10,12), and determining the SMA branching pattern can assist surgeons in quickly ligating branches, avoiding prolonged surgery time and inadvertent ligation of vessels due to the absence of certain branches (14-16). Moreover, postoperative persistent diarrhea is often due to damage to the superior mesenteric artery plexus (SMAP) during surgery, which typically resides within the SMA perivascular sheath and surrounds the SMA and its branches. Therefore, precise ligation of SMA branch vessels can reduce the incidence of this complication.

Traditional computed tomography (CT) angiography uses mixed energy X-ray to visualize small vascular branches. However, beam hardening effects significantly reduce image sharpness and contrast. Although increasing the concentration of contrast agent can enhance image quality, it imposes a great burden on patients and increases the risk of adverse reactions.

With advancements in imaging technology, new CT models and post-processing reconstruction techniques have been developed to address these limitations. These include dual detector spectral CT, which captures high- and low-energy X-ray photons through the bilateral detector structure; dual source dual energy CT, which acquires data simultaneously from A and B X-ray tubes and the same anatomical level; and single source dual-energy CT, which uses instantaneous tube voltage switching via a high-voltage generator to achieve spectral imaging (17-19). Although these spectral CT systems differ in their scanning methods, they share the same principle: by exploiting differences in X-ray attenuation at different energy levels, they enable material separation and quantitative analysis. Based on this principle, new post-processing technologies, such as virtual non-contrasting imaging, iodine density mapping, and virtual monoenergetic imaging, have been developed to optimize image quality, assess material composition, and improve diagnostic accuracy (20). Virtual monoenergetic imaging can generate single-energy images at 40–200 kiloelectron volt (keV). Low energy images enhance contrast and improve visualization of small blood vessels while simultaneously reducing image noise (20). Lai *et al.* (21) found that 60 keV virtual monoenergetic images provided superior visualization of the SMA while allowing a reduction in contrast agent

Highlight box

Key findings

- We optimized the display of the superior mesenteric artery using dual energy computed tomography (CT) three-dimensional (3D) reconstruction and arterial venous image fusion technology, and further evaluated its anatomical variations in the clinical value of laparoscopic right hemicolectomy for colon cancer.

What is known and what is new?

- Spectral CT can optimize the display of variations in the branches of the superior mesenteric artery.
- The anatomical variations of the superior mesenteric artery displayed by CT 3D reconstruction and image fusion technology are helpful for clinicians to formulate individualized laparoscopic right hemicolectomy plans.

What is the implication, and what should change now?

- We used dual energy CT 3D reconstruction and arterial venous image fusion technology to quickly and accurately evaluate the anatomical characteristics of superior mesenteric artery (SMA) and the relationship between the right branch blood vessels and superior mesenteric vein, providing guidance for developing personalized surgical plans with SMA as the priority approach for patients with laparoscopic right colon cancer.

concentration and injection rate.

In addition, three-dimensional (3D) reconstruction technology provides a more 3D display of abdominal organs and blood vessel morphology, and image fusion technology can combine vascular images from different phases. The use of these 3D imaging techniques facilitates the preoperative evaluation of abdominal vascular anatomical characteristics (5,22,23).

Most current literature focuses on the branching patterns of the SMA or explores the impact of specific SMA anatomical features on related diseases. This study aims to comprehensively investigate the clinical significance of SMA branching patterns, root positions, distances between branch roots, and the relationship between right branch vessels and the SMV in laparoscopic radical right hemicolectomy for right colon cancer using spectral CT 3D reconstruction and image fusion technology, providing relevant references for clinicians in formulating rational surgical plans. We present this article in accordance with the STROBE reporting checklist (available at https://jgo.amegroups.com/article/view/10.21037/jgo-2025-167/rc).

Methods

Study subjects

A retrospective analysis was conducted of clinical and imaging data from patients with pathologically confirmed right colon cancer who underwent enhanced abdominal and pelvic spectral CT before surgery at the Department of Medical Imaging, Affiliated Hospital of Nantong University from January 2020 to June 2024. This study was approved by the Ethics Committee of Affiliated Hospital of Nantong University (approval No. 2024-K132-01). The study was conducted in accordance with the Declaration of Helsinki and its subsequent amendments. As a retrospective study, informed consent from patients was not required.

Inclusion criteria: (I) patients who underwent enhanced spectral CT of the whole abdomen and pelvis before surgery; (II) patients with complete clinical data.

Exclusion criteria: (I) cases where SMA anatomical measurements were affected by embolism, intramural hematoma, or severe atherosclerosis; (II) patients with a history of abdominal surgery involving the SMA; (III) patients with acute abdomen conditions such as bowel obstruction or perforation requiring open surgery; (IV) patients with spinal abnormalities or a history of lumbar disc surgery; (V) cases where image quality was compromised by significant ascites.

A total of 64 cases were excluded for various reasons: 28 cases due to embolism, intramural hematoma, or severe atherosclerosis affecting SMA anatomical measurements; 14 cases requiring open surgery due to acute abdomen conditions like bowel obstruction or perforation; 7 cases with severe spinal abnormalities; 11 cases with a history of abdominal intestinal surgery; and 4 cases where image quality was affected by significant ascites. Ultimately, 316 patients were included in the study.

Scanning protocol and reconstruction methods

The scanning was performed using a Siemens dual-energy CT scanner (Somatom Force, Siemens Healthcare, Forchheim, Germany). Scanning protocol: Patients were positioned supine with hands raised above the head, scanning from the diaphragm to the symphysis pubis. Scanning parameters: Tube voltage was 120 kV for the A tube and Sn150 kV for the B tube, with tube currents of 150 mAs for the A tube and 90 mAs for the B tube, a linear fusion coefficient of 0.5, pitch of 1.0, rotation speed of 0.5 seconds per rotation, and a slice thickness of 5 mm. Contrast agent: Iopromide with a concentration of 370 mgI/mL was administered at a rate of 3.5 mL/s, with a dose of approximately 70–90 mL, followed by about 20 mL of saline. Dual-phase scanning was performed, with the arterial phase triggered at an aortic threshold of 110 Hounsfield units (HU) at the T11 vertebra, followed by a venous phase scan 40 seconds later.

Image post-processing

After scanning, the enhanced CT images of the whole abdomen and pelvis in the arterial and venous phases were transmitted to the Synovia post-processing workstation and the IntelliSpace Portal workstation. Using post-processing 3D reconstruction techniques, axial images with a slice thickness and interval of 1mm were obtained for multi-planar reconstruction (MPR), thin-slice maximum intensity projection (thin-MIP), and curved planar reformation (CPR) images. The SMA and SMV were reconstructed using thin-MIP in an oblique sagittal plane (parallel to the SMA long axis, slice thickness of 10 mm, interval of 3 mm), and the lengths between the roots of SMA branches were measured using CPR images. 3D images of the SMA were obtained using volume rendering (VR) reconstruction, retaining the lumbar spine. The SMA and SMV were

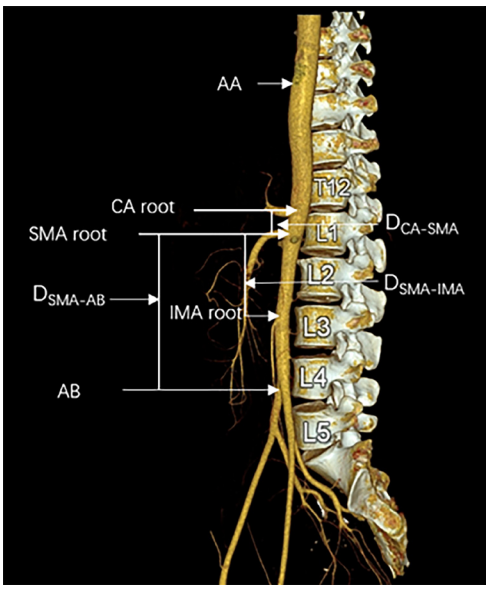

Figure 1 Fusion image of celiac blood vessels and spine. Using volume rendering technology to determine the vertebral level of the SMA root and to measure D_{CA-SMA}, $D_{SMA-IMA}$, and D_{SMA-AB}. D_{CA-SMA}: the vertical distance from the root of the CA to the root of the SMA. $D_{SMA-IMA}$: the vertical distance from the root of the SMA to the root of the IMA. D_{SMA-AB}: the distance from the root of the SMA to the AB. AA, abdominal aorta; AB, bifurcation of the abdominal aorta; CA, celiac artery; IMA, inferior mesenteric artery; SMA, superior mesenteric artery.

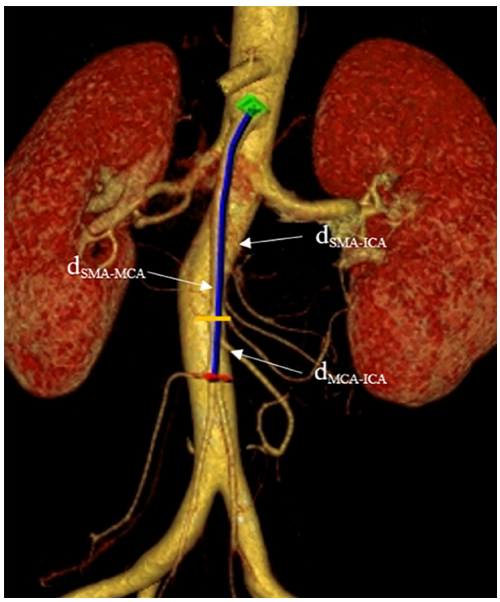

Figure 2 Distance measurement image of the right branch root of the SMA. Green marker: root of the SMA; yellow marker: root of the MCA; red marker: root of the ICA. $d_{SMA-MCA}$: distance from the root of the SMA to the root of the MCA. $d_{SMA-ICA}$: distance from the root of the SMA to the root of the ICA. $d_{MCA-ICA}$: distance from the root of the MCA to the root of the ICA. ICA, ileocolic artery; MCA, middle colic artery; SMA, superior mesenteric artery.

fused into a single image using arteriovenous image fusion techniques.

Measurement methods

Two radiologists with 3 and 5 years of abdominal imaging experience respectively reviewed the images together. On the VR images, they measured the vertical distance from the root of the SMA to the root of the celiac artery (CA) (D_{CA-SMA}), the vertical distance from the root of the SMA to the root of the inferior mesenteric artery (IMA) ($D_{SMA-IMA}$), and the distance from the root of the SMA to the abdominal aorta bifurcation (AB) (D_{SMA-AB}), as shown in *Figure 1*. On the CPR images, they measured the distance from the root of the SMA to the root of the middle colic artery (MCA) ($d_{SMA-MCA}$), the distance from the root of the SMA to the root of the ICA ($d_{SMA-ICA}$), and the distance from the root of the MCA to the root of the ICA ($d_{MCA-ICA}$), as shown in *Figure 2*. Each measurement was repeated three times, and the average value was taken.

When determining the branching pattern of the SMA on VR and thin-MIP images, due to significant variations in SMA branches, this study primarily identified the branching pattern of vessels supplying the right half of the colon (MCA, RCA, ICA). The positional relationship between the right branch vessels of the SMA and the SMV was assessed on thin-layer arterial and venous axial images and arterial-venous fusion images.

Statistical analysis

Statistical analysis was performed using SPSS 26.0 software. Quantitative data between two groups were compared using independent samples *t*-tests. Multiple group comparisons utilized one-way analysis of variance (ANOVA), with Tukey's post hoc test for pairwise comparisons. Categorical count data between two groups were analyzed using the Pearson's Chi-squared test. The relationship between ICA and SMV anatomical pathways with clinical characteristics was assessed using single-factor analysis. Multiple logistic regression analyzed gender, $d_{SMA-ICA}$, $d_{MCA-ICA}$, and their

Table 1 Baseline clinical characteristics

Group	Values (N=316)
Age (years)	59.53±10.46
Gender	
Male	187 (59.18)
Female	129 (40.82)
Height (cm)	166.22±7.27
Weight (kg)	66.37±11.22
BMI (kg/m^2)	23.97±3.42
Tumor location	
Cecum	31 (9.81)
Ascending colon	181 (57.28)
Hepatic flexure	45 (14.24)
Transverse colon (right third)	59 (18.67)

Data are presented as n (%) or $\bar{x}$±s. BMI, body mass index.

positions. Statistical significance was set at P<0.05 for all tests, indicating significant differences.

Results

Clinical data results

A total of 380 patients were included in this study, and 316 patients were finally included according to the inclusion and exclusion criteria (187 males, age range 34 to 84 years, mean age 60.07±10.01 years; 129 females, age range 33 to 84 years, mean age 58.74±11.07 years). See *Table 1* for details.

Relationship between SMA root position and clinical characteristics

Relationship between SMA root position and vertebral level

In this study of 316 cases, the analysis revealed the following distribution of SMA root origins in relation to vertebral levels: SMA originated at the level of T12 vertebra in 21 cases, accounting for approximately 6.65%. SMA originated at the level of T12/L1 intervertebral disc in 29 cases, approximately 9.18%. SMA originated at the level of L1 vertebra in 236 cases, the highest proportion at approximately 74.68%. SMA originated at the level of L2/L1 intervertebral disc in 24 cases, approximately 7.59%. IMA originated at the level of L2 vertebra in 6 cases, the lowest proportion at 1.90%, and at the lowest vertebral level.

The vertical distances from the SMA root to the celiac artery (CA) root ($D_{CA\text{-}SMA}$) were measured at 18.67±4.36 mm. Among these, 2 cases were identified where the CA and SMA shared a common trunk originating from the abdominal aorta. The vertical distance from the SMA root to the IMA root ($D_{SMA\text{-}IMA}$) was 73.26±10.01 mm, and the distance from the SMA root to the AB ($D_{SMA\text{-}AB}$) was 115.97±11.82 mm. Further analysis of the relationship between the SMA root position and vertebral level in the 316 cases revealed no statistically significant differences in $D_{CA\text{-}SMA}$, $D_{SMA\text{-}IMA}$, and $D_{SMA\text{-}AB}$ distances (P>0.05).

Relationship between SMA root position, branch root distances, and patient clinical characteristics

In this study, the distances measured were: SMA root to MCA root ($d_{SMA\text{-}MCA}$): 62.70±12.10 mm; SMA root to ICA root ($d_{SMA\text{-}ICA}$): 87.82±13.85 mm; MCA root to ICA root ($d_{MCA\text{-}ICA}$): 25.12±10.59 mm.

Additionally, we assessed the relationship between SMA root position, branch root distances, and patient characteristics (*Table 2*). Patients were categorized into four groups based on gender and BMI levels, revealing that males with higher BMI had a significantly greater distance in $D_{SMA\text{-}AB}$ (F=4.961, P=0.002).

Branching patterns of SMA

In this study, the presence rates were 100% for MCA and ICA. RCA exhibited higher variability, present in only 126 cases, accounting for approximately 39.87%. Based on the classification by Yada *et al.* [1997] (24) concerning the right branch of the SMA, this study categorized SMAs with and without RCA. SMAs with RCA were classified as Type I, further divided into three subtypes: Type Ia SMA (independent origins of MCA, RCA, and ICA) with 99 cases, approximately 31.33%; Type Ib SMA (shared origin of RCA and MCA) with 16 cases, approximately 5.06%; Type Ic SMA (shared origin of RCA and ICA) with 11 cases, approximately 3.48%. SMAs lacking RCA were categorized as Type II SMA, comprising 190 cases, approximately 60.13% (*Figure 3*).

Further analysis of SMA types and their relationship with $d_{SMA\text{-}MCA}$, $d_{SMA\text{-}ICA}$, and $d_{MCA\text{-}ICA}$ distances revealed the following findings: There were no statistically significant differences in $d_{SMA\text{-}MCA}$ and $d_{SMA\text{-}ICA}$ among the four

Table 2 Relationship between SMA root position, distances between branch roots, and patient characteristics (mm, $\bar{x} \pm s$)

Distance	Male		Female		F value	P value
	BMI ≤25 kg/m^2	BMI >25 kg/m^2	BMI ≤25 kg/m^2	BMI >25 kg/m^2		
D_{CA-SMA}	18.47±4.99	19.47±4.22	19.01±3.39	17.30±4.15	2.449	0.06
$D_{SMA-IMA}$	72.97±8.55	75.40±12.78	71.75±9.75	73.80±9.26	1.748	0.16
D_{SMA-AB}	116.00±10.10	120.43±14.54	113.47±11.91	114.07±9.75	4.961	0.002
$d_{SMA-MCA}$	12.36±1.12	11.89±1.46	11.76±1.27	12.26±1.87	1.179	0.32
$d_{SMA-ICA}$	87.00±14.54	90.18±15.03	87.20±12.99	87.75±11.52	0.835	0.48
$d_{MCA-ICA}$	10.75±0.98	11.88±1.46	9.18±0.99	10.49±1.60	1.487	0.22

D_{CA-SMA}: the vertical distance from the root of the CA to the root of the SMA. $D_{SMA-IMA}$: the vertical distance from the root of the SMA to the root of the IMA. D_{SMA-AB}: the distance from the root of the SMA to the AB. $d_{SMA-MCA}$: distance from the root of the SMA to the root of the MCA. $d_{SMA-ICA}$: distance from the root of the SMA to the root of the ICA. $d_{MCA-ICA}$: distance from the root of the MCA to the root of the ICA. AB, bifurcation of the abdominal aorta; BMI, body mass index; CA, celiac artery; ICA, ileocolic artery; IMA, inferior mesenteric artery; MCA, middle colic artery; SMA, superior mesenteric artery.

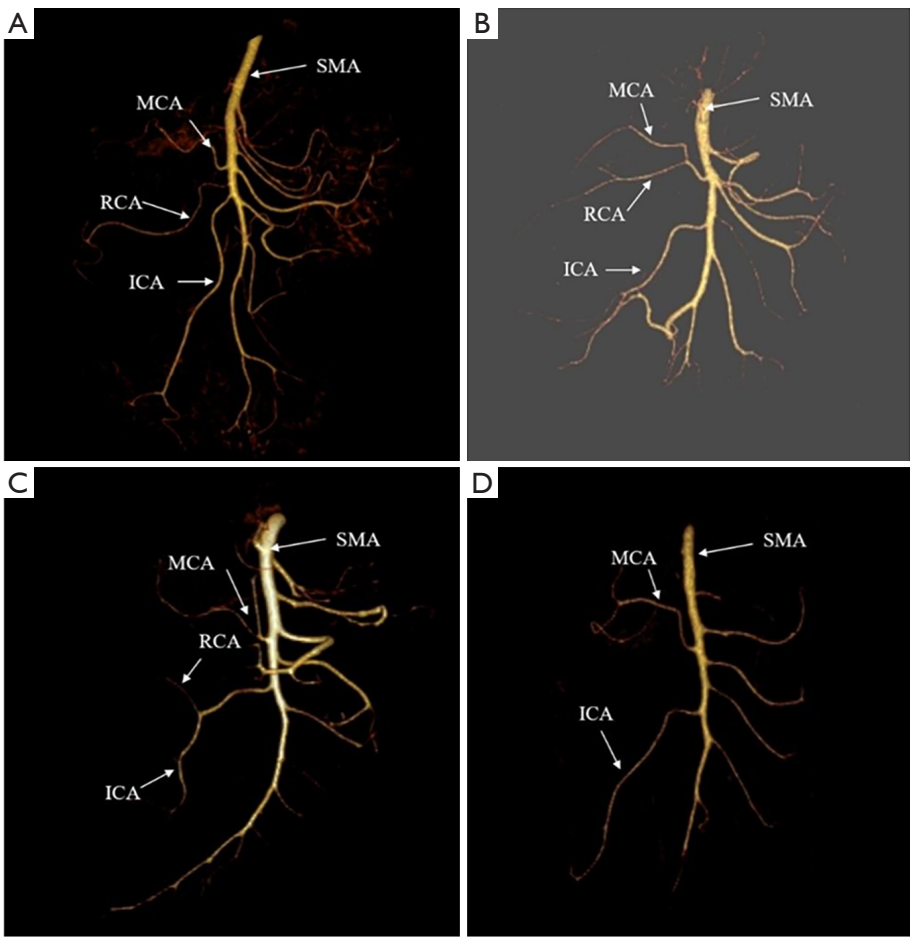

Figure 3 Volume rendering image of the SMA. Types of right branches of the SMA. (A) Type Ia. (B) Type Ib. (C) Type Ic. (D) Type II. ICA, ileocolic artery; MCA, middle colic artery; RCA, right colic artery; SMA, superior mesenteric artery.

Table 3 Relationship between different SMA types and distances between main trunk roots and branch roots (mm, $\bar{x} \pm s$)

Distance	Type I SMA			Type II SMA	F value	P value
	Type Ia SMA	Type Ib SMA	Type Ic SMA			
$d_{SMA-MCA}$	62.45±11.00	64.25±15.42	65.18±10.90	62.56±12.47	0.262	0.85
$d_{SMA-ICA}$	90.05±14.68	89.46±11.65	85.87±8.60	86.64±13.74	1.469	0.22
$d_{MCA-ICA}$	27.60±11.67	25.23±8.81	20.69±7.38	24.08±10.10	3.117	0.03

$d_{SMA-MCA}$: distance from the root of the SMA to the root of the MCA. $d_{SMA-ICA}$: distance from the root of the SMA to the root of the ICA. $d_{MCA-ICA}$: distance from the root of the MCA to the root of the ICA. ICA, ileocolic artery; MCA, middle colic artery; SMA, superior mesenteric artery.

Table 4 Relationship between Type I and Type II SMA branch root distances (mm, $\bar{x} \pm s$)

Distance	Type I SMA	Type II SMA	t value	P value
$d_{MCA-ICA}$	26.69±11.16	24.08±10.10	–2.159	0.032

$d_{MCA-ICA}$: distance from the root of the MCA to the root of the ICA. ICA, ileocolic artery; MCA, middle colic artery; SMA, superior mesenteric artery.

SMA types. However, there was a statistically significant difference in $d_{MCA-ICA}$ (F=3.117, P=0.03). The distances for $d_{MCA-ICA}$ in Types Ia, Ib, Ic, and II SMA were 27.60±11.67, 25.23±8.81, 20.69±7.38, and 24.08±10.10 mm, respectively. Subsequently, after combining the three subtypes into Type I SMA, the $d_{MCA-ICA}$ distance was 26.69±11.16 mm, which was longer than the 24.08±10.10 mm observed in Type II SMA (t=–2.159, P=0.03) (*Tables 3*,*4*).

Relationship between MCA, RCA, ICA, and SMV pathways

Among the 316 cases included in this study, five distinct pathways were identified and categorized as follows (*Figure 4*): Type A1: MCA, RCA, and ICA running anterior to SMV, totaling 65 cases, approximately 20.57%. Type A2: MCA and RCA running anterior to SMV, while ICA runs posterior to SMV, totaling 50 cases, approximately accounting for 15.83%. Type A3: MCA runs anterior to SMV, while RCA and ICA run posterior to SMV, totaling 11 cases, approximately 3.48%. Type B1: RCA absent, MCA and ICA running anterior to SMV, totaling 95 cases, approximately 30.06%. Type B2: RCA absent, MCA runs anterior to SMV, while ICA runs posterior to SMV, totaling 95 cases, approximately accounting for 30.06%.

Among these cases, MCA running anterior to SMV accounted for 100%. When RCA was present, it ran anterior to SMV in approximately 91.27% (115/126) of cases. ICA running anterior to SMV accounted for approximately 50.63% (160/316). In cases where RCA ran posterior to SMV, no instances of ICA running anterior to SMV were observed.

We further evaluated the relationship between ICA pathway and SMV, as well as clinical characteristics of the study subjects (*Tables 5*,*6*). It was found that ICA running anterior to SMV was significantly associated with male gender, shorter distances of $d_{SMA-ICA}$ and $d_{MCA-ICA}$ (t/χ^2 values were 9.293, –2.326, –3.191; P values were 0.002, 0.02, 0.002 respectively). However, ICA pathway (anterior or posterior to SMV) showed no significant correlation with age, height, weight, body mass index (BMI), D_{CA-SMA}, $D_{SMA-IMA}$, D_{SMA-AB}, $d_{SMA-MCA}$, or the presence of RCA (P>0.05) (*Table 5*).

Based on the above analysis, gender, $d_{SMA-ICA}$, and $d_{MCA-ICA}$ were included to construct a multiple logistic regression model. The results indicated that gender and $d_{MCA-ICA}$ were independent influencing factors for the different positions of ICA running anterior or posterior to SMV [odds ratio (OR) =0.499, 95% confidence interval (CI): 0.314–0.794, P=0.003 for gender; OR =1.027, 95% CI: 1.001–1.005, P=0.042 for $d_{MCA-ICA}$] (*Table 6*).

Discussion

Hohenberger *et al.* (25) established the theoretical basis and operational standards for CME in radical surgery for right-sided colon cancer. The core principle involves sharp dissection between the visceral and parietal layers of the peritoneum, complete excision of the mesocolic roots

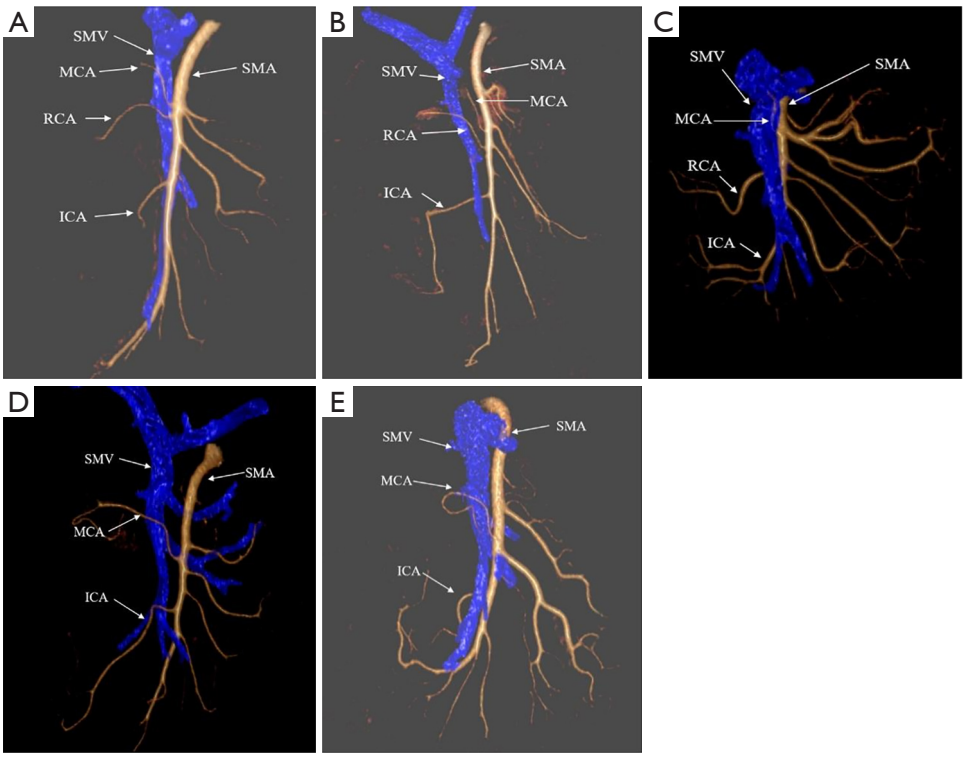

Figure 4 Fusion image of the SMA and SMV. Relationship between the right branch vessels of the SMA and the SMV. (A) Type A1. (B) Type A2. (C) Type A3. (D) Type B1. (E) Type B2. ICA, ileocolic artery; MCA, middle colic artery; RCA, right colic artery; SMA, superior mesenteric artery; SMV, superior mesenteric vein.

and anterior and posterior fasciae, high ligation of blood vessels, and thorough clearance of regional lymph nodes (including lymph nodes at the roots of the MCA, RCA, and ICA). However, current guidelines such as those from the National Comprehensive Cancer Network (NCCN) (26), the European Society for Medical Oncology (ESMO) (27), the Japanese Society for Cancer of the Colon and Rectum (JSCCR) (28), and the Chinese Guidelines for Diagnosis and Treatment of Colorectal Cancer (2023 edition) (29) do not provide explicit instructions regarding the medial margin of lymph node clearance in radical surgery for right-sided colon cancer. The choice of medial margin affects the thoroughness of regional lymph node clearance and subsequently impacts patient prognosis.

Currently, the majority of scholars (30) consider the left margin of the SMV as the medial margin for lymph node clearance in radical surgery for right-sided colon cancer. This approach partly achieves mesocolic excision and regional lymph node clearance. However, according to the principles of CME, mesocolic excision must extend to the root of the SMA, and central lymph nodes also exist anterior to the SMA, which cannot be achieved with standard SMV-based lymph node clearance alone. As a result, some scholars (10,12) have shifted focus from the SMV to the SMA, adopting an "SMA-first" approach for radical resection of right-sided colon cancer. This approach involves using the midline or left margin of the SMA as the medial margin for lymph node clearance. However, due to significant anatomical variations in the right-sided branches of the SMA and their deep position relative to adjacent mesocolon and vessels, determining the precise location of the SMA, analyzing the anatomical characteristics of its branches, and accurately ligating vessels during laparoscopic procedures pose significant challenges for colorectal surgeons. Therefore, preoperative use of 3D imaging reconstruction techniques to understand the anatomical features of the SMA and the course of its branches relative to the SMV is of paramount importance.

To quickly and accurately locate the SMA as the initial step in radical surgery for right-sided colon cancer, some surgical techniques (12) involve a "caudal approach" to dissect the mesentery towards the ileocecal area and identify

Table 5 Relationship between ICA pathway and SMV with clinical characteristics

Group	ICA pathway posterior to SMV	ICA pathway anterior to SMV	t/χ^2 value	P value
Gender			9.293	0.002
Male	108 (67.5)	79 (50.6)		
Female	52 (32.5)	77 (49.4)		
Age (years)	60.60±9.80	58.44±11.03	1.845	0.07
Height (cm)	166.39±7.29	166.04±7.26	0.426	0.67
Weight (kg)	66.59±11.06	66.14±11.41	0.354	0.72
BMI (kg/m^2)	23.97±3.17	23.96±3.66	0.034	0.97
D_{CA-SMA} (mm)	18.40±4.79	18.94±3.86	–1.092	0.28
$D_{SMA-IMA}$ (mm)	73.42±9.54	73.09±10.59	0.289	0.77
D_{SMA-AB} (mm)	115.87±11.41	116.08±12.27	–0.157	0.88
$d_{SMA-MCA}$ (mm)	62.87±12.91	62.69±11.95	0.133	0.89
$d_{SMA-ICA}$ (mm)	86.05±13.97	89.65±13.53	–2.326	0.02
$d_{MCA-ICA}$ (mm)	23.17±11.03	26.96±9.99	–3.191	0.002
RCA presence (case)			0.398	0.82
Type I	65 (40.6)	61 (39.1)		
Type II	95 (59.4)	95 (60.9)		

Data are presented as n (%) or $\bar{x}$ ± s. D_{CA-SMA}: the vertical distance from the root of the CA to the root of the SMA. $D_{SMA-IMA}$: the vertical distance from the root of the SMA to the root of the IMA. D_{SMA-AB}: the distance from the root of the SMA to the AB. $d_{SMA-MCA}$: distance from the root of the SMA to the root of the MCA. $d_{SMA-ICA}$: distance from the root of the SMA to the root of the ICA. $d_{MCA-ICA}$: distance from the root of the MCA to the root of the ICA. AB, bifurcation of the abdominal aorta; BMI, body mass index; CA, celiac artery; ICA, ileocolic artery; IMA, inferior mesenteric artery; MCA, middle colic artery; RCA, right colic artery; SMA, superior mesenteric artery; SMV, superior mesenteric vein.

Table 6 Correlation between ICA pathway and SMV with multifactorial clinical characteristics

Group	B value	SE value	Wald value	OR value	95% CI	P value
Gender	–0.685	0.237	8.599	0.499	0.314–0.794	0.003
$d_{SMA-ICA}$	0.010	0.010	0.943	1.010	0.990–1.030	0.33
$d_{MCA-ICA}$	0.027	0.774	4.139	1.027	1.001–1.005	0.042

$d_{SMA-ICA}$: distance from the root of the SMA to the root of the ICA. $d_{MCA-ICA}$: distance from the root of the MCA to the root of the ICA. CI, confidence interval; ICA, ileocolic artery; MCA, middle colic artery; OR, odds ratio; SE, standard error; SMA, superior mesenteric artery; SMV, superior mesenteric vein.

the ICA to determine the SMA's position. However, this method has inherent localization inaccuracies. Conversely, starting from the cranial end to identify anatomical landmarks and using a bilateral approach from both ends can enhance the accuracy of SMA localization. This study found that in the majority of cases (74.68%), the SMA root is located at the level of the L1 vertebra, between the T12 and L2 vertebrae. Specific measurements showed that the average distance from the SMA root to the SMV was 18.67±4.36 mm, to the IMA root was 73.26± 10.01 mm, and to the AB was 115.97±11.82 mm. These measurements are largely consistent with previous studies (15,31,32) (18.40±4.30, 72.96±9.75, 109.40±0.96 mm respectively).

Further analysis of these distances in relation to vertebral levels, gender, and BMI revealed that D_{CA-SMA}, $D_{SMA-IMA}$,

and D_{SMA-AB} did not show statistically significant differences (P>0.05). However, distances from the SMA root to the AB were longer in males and individuals with higher BMI. These measurements assist surgeons in preoperative planning by determining the vertebral level of the SMA root and measuring D_{SMA-AB} for accurate SMA cranial end localization. Additionally, this study measured the average distance of $d_{MCA-ICA}$ as 25.12±10.59 mm, which closely aligns with other studies [e.g., Grytsenko *et al.* (8) reported an average of 29.5±15.7 mm]. Further analysis of different types of SMA right-side branches and their relationship with $d_{MCA-ICA}$ showed that the distance in Type I SMA (with RCA present) was longer (26.69±11.16 mm) than in Type II SMA (RCA absent) (24.08±10.10 mm). These measurements facilitate surgeons in estimating distances and time required for effectively handling vessels and clearing lymph nodes during ICA upward processing.

After determining the position of SMA, vascular ligation along with regional lymph node dissection is performed upwards along the ICA. Preoperative familiarity with the patterns of SMA right-side branches is crucial to avoid prolonged surgical time due to the absence of specific vessels (8,13,15). This study categorized SMA right-side branches based on the presence or absence of the right colic artery (RCA), which has a higher variability and significant impact on right-sided colon surgeries. The SMA Type I with RCA present accounted for only 39.87%, while Type II without RCA accounted for 60.13%, aligning closely with Murono *et al.*'s findings (33) (33.4%, 66.6%). We further subdivided Type I into three subtypes: Type Ia SMA was the most prevalent at 31.33%, followed by Type Ib at approximately 5.06%, and Type Ic at about 3.48%. Previous literatures (15,34,35) have reported additional subtypes, including variations such as accessory MCA arising from Type Ia or Ic, the origin of left and right branches of the MCA from the SMA trunk, and the left colic artery arising from the MCA. A study (35) also includes the inferior pancreaticoduodenal artery originating from the SMA in their branch pattern evaluations, which were not mentioned in this study. This omission is partly due to the minor impact of variations in vessels such as the inferior pancreaticoduodenal artery supplying pancreatic blood flow or the left colic artery supplying the left half of the colon on the "SMA-first approach" for radical right-sided colon cancer surgery. Furthermore, some smaller branch vessels are difficult to display in CT 3D reconstructions.

In "SMA-first" approach surgeries, the SMA often runs behind the SMV, posing significant challenges during dissection. Preoperative understanding of the course of SMA right-side branches relative to the SMV can provide crucial information to surgeons, helping to prevent inadvertent vascular injury and intraoperative bleeding (10,12). This study found that all MCAs run exclusively on the ventral side of the SMV, while only 8.27% of RCAs run on the dorsal side of the SMV. In cases where RCA runs dorsally, the inferior colic artery (ICA) consistently runs dorsally as well, corroborating findings from Murono *et al.* (33) and Nigah *et al.* (15). Furthermore, this study identified gender and the distance between the MCA and the inferior colic artery ($d_{MCA-ICA}$) as independent factors influencing the location of ICA running along the SMV. In males and those with shorter $d_{MCA-ICA}$ distances, there is a higher incidence of ICA running ventrally along the SMV. Preoperative knowledge of the relationship between SMA right-side branches and the SMV facilitates precise vascular ligation by surgeons.

There are several limitations in this study: (I) it did not compare the anatomical characteristics of the SMA depicted in 3D reconstructions with the actual intraoperative findings to validate the accuracy of CT 3D reconstruction technology; (II) it did not further analyze the patterns of SMA right-side branches and their relationship with SMV course, which could have specific implications for intraoperative and postoperative outcomes in patients with right-sided colon cancer. Future work: we plan to integrate artificial intelligence (AI) technology with imaging techniques to better study anatomical variations of the SMA. Building on previous work using AI for semi-automatic quantitative grading of SMA, we aim to apply this technology in clinical practice to assist surgeons during operations and ultimately improve patient outcomes.

Conclusions

The above analysis indicates that spectral CT 3D reconstruction and fusion imaging of arterial and venous maps can rapidly and accurately assess the position of the SMA root, the vascular pattern of its right branches, the distances between various branch roots, and their relationship with the SMV. This helps in devising a rational surgical approach, prioritizing the SMA, for laparoscopic surgery in patients with right-sided colon cancer.

Acknowledgments

None.

Footnote

Reporting Checklist: The authors have completed the STROBE reporting checklist. Available at https://jgo.amegroups.com/article/view/10.21037/jgo-2025-167/rc

Data Sharing Statement: Available at https://jgo.amegroups.com/article/view/10.21037/jgo-2025-167/dss

Peer Review File: Available at https://jgo.amegroups.com/article/view/10.21037/jgo-2025-167/prf

Funding: This work was supported by grants from the Young Scientists Fund of the National Natural Science Foundation of China (grant No. 81901738) and Nantong Science and Technology Planning Project (grant No. MS22022061).

Conflicts of Interest: All authors have completed the ICMJE uniform disclosure form (available at https://jgo.amegroups.com/article/view/10.21037/jgo-2025-167/coif). The authors have no conflicts of interest to declare.

Ethical Statement: The authors are accountable for all aspects of the work in ensuring that questions related to the accuracy or integrity of any part of the work are appropriately investigated and resolved. The study was conducted in accordance with the Declaration of Helsinki and its subsequent amendments. This study was approved by the Ethics Committee of Affiliated Hospital of Nantong University (approval No. 2024-K132-01). As a retrospective study, informed consent from patients was not required.

References

1. Nesgaard JM, Stimec BV, Bakka AO, et al. Navigating the mesentery: a comparative pre- and per-operative visualization of the vascular anatomy. Colorectal Dis 2015;17:810-8.
2. Yang JS, Xu ZY, Chen FX, et al. Role of clinical data and multidetector computed tomography findings in acute superior mesenteric artery embolism. World J Clin Cases 2022;10:4020-32.
3. Ghodasara N, Liddell R, Fishman EK, et al. High-Value Multidetector CT Angiography of the Superior Mesenteric Artery: What Emergency Medicine Physicians and Interventional Radiologists Need to Know. Radiographics 2019;39:559-77.
4. Kuzu MA, İsmail E, Çelik S, et al. Variations in the Vascular Anatomy of the Right Colon and Implications for Right-Sided Colon Surgery. Dis Colon Rectum 2017;60:290-8.
5. Bian L, Wu D, Chen Y, et al. Clinical Value of Multi-Slice Spiral CT Angiography, Colon Imaging, and Image Fusion in the Preoperative Evaluation of Laparoscopic Complete Mesocolic Excision for Right Colon Cancer: a Prospective Randomized Trial. J Gastrointest Surg 2020;24:2822-8.
6. Li K, Cao F, He X, et al. The concept of developmental anatomy: the greater omentum should be resected in right-sided colon cancer? BMC Surg 2023;23:137.
7. Wang X, Ni H, Jia W, et al. Value of different anastomoses in laparoscopic radical right hemicolectomy for right-sided colon cancer: retrospective study and literature review. World J Surg Oncol 2022;20:318.
8. Grytsenko S, Dzyubanovsky I, Hrytsenko I, et al. Preoperative computed tomography angiography in multidisciplinary personalized assessment of patient with right-sided colon cancer: surgeon and radiologist point of view. Arq Bras Cir Dig 2022;35:e1679.
9. Sun Y, Feng Y, Zhang D, et al. Application value of superior mesenteric artery-oriented complete mesocolic excision in the treatment of right colon cancer. Chin J Digest Surg 2019;18:753-60.
10. Yi X, Li H, Lu X, et al. "Caudal-to-cranial" plus "artery first" technique with beyond D3 lymph node dissection on the right midline of the superior mesenteric artery for the treatment of right colon cancer: is it more in line with the principle of oncology? Surg Endosc 2020;34:4089-100.
11. Wang Y, Zhang D, Feng Y, et al. Clinical efficacy of superior mesenteric artery-oriented laparoscopic complete mesocolic excision in the treatment of right colonic cancer. Zhonghua Wei Chang Wai Ke Za Zhi 2017;20:896-9.

12. Luo W, Cai Z, Li F, et al. Laparoscopic Complete Mesocolic Excision with Central Vascular Ligation (CME + CVL) for Right-Sided Colon Cancer: A New "Superior Mesenteric Artery First" Approach. Ann Surg Oncol 2022;29:5066-73.
13. Cirocchi R, Randolph J, Davies RJ, et al. A systematic review and meta-analysis of variants of the branches of the superior mesenteric artery: the Achilles heel of right hemicolectomy with complete mesocolic excision? Colorectal Dis 2021;23:2834-45.
14. Taha KM, Karrar Alsharif MH, Elamin AY. Variation in morphology and branching pattern of superior mesenteric artery. Folia Morphol (Warsz) 2017;76:532-5.
15. Nigah S, Patra A, Chumbar S, et al. Topographic location and branching pattern of the superior mesenteric artery with its clinical relevance: a cadaveric study. Folia Morphol (Warsz) 2022;81:372-8.
16. Luzon JA, Thorsen Y, Nogueira LP, et al. Reconstructing topography and extent of injury to the superior mesenteric artery plexus in right colectomy with extended D3 mesenterectomy: a composite multimodal 3-dimensional analysis. Surg Endosc 2022;36:7607-18.
17. Lai LY, Jiang Y, Shu J. The Application of Dual-layer Spectral Detector CT in Abdominal Vascular Imaging. Curr Med Imaging 2023;19:1609-15.
18. Remy-Jardin M, Guiffault L, Oufriche I, et al. Image quality of lung perfusion with photon-counting-detector CT: comparison with dual-source, dual-energy CT. Eur Radiol 2024;34:7831-44.
19. Wang J, He Y, Yan L, et al. Predicting Osteoporosis and Osteopenia by Fusing Deep Transfer Learning Features and Classical Radiomics Features Based on Single-Source Dual-energy CT Imaging. Acad Radiol 2024;31:4159-70.
20. McCollough CH, Leng S, Yu L, et al. Dual- and Multi-Energy CT: Principles, Technical Approaches, and Clinical Applications. Radiology 2015;276:637-53.
21. Lai LY, Tan P, Jiang Y, et al. Dual-layer spectral detector CT for contrast agent concentration, dose and injection rate reduction: Utility in imaging of the superior mesenteric artery. Eur J Radiol 2022;150:110246.
22. Liu LP, Shapira N, Halliburton SS, et al. Spectral performance evaluation of a second-generation spectral detector CT. J Appl Clin Med Phys 2024;25:e14300.
23. Beeres M, Trommer J, Frellesen C, et al. Evaluation of different keV-settings in dual-energy CT angiography of the aorta using advanced image-based virtual monoenergetic imaging. Int J Cardiovasc Imaging 2016;32:137-44.
24. Yada H, Sawai K, Taniguchi H, et al. Analysis of vascular anatomy and lymph node metastases warrants radical segmental bowel resection for colon cancer. World J Surg 1997;21:109-15.
25. Hohenberger W, Weber K, Matzel K, et al. Standardized surgery for colonic cancer: complete mesocolic excision and central ligation--technical notes and outcome. Colorectal Dis 2009;11:354-64; discussion 364-5.
26. Schmoll HJ, Van Cutsem E, Stein A, et al. ESMO Consensus Guidelines for management of patients with colon and rectal cancer. a personalized approach to clinical decision making. Ann Oncol 2012;23:2479-516.
27. Daly MB, Pal T, Berry MP, et al. Genetic/Familial High-Risk Assessment: Breast, Ovarian, and Pancreatic, Version 2.2021, NCCN Clinical Practice Guidelines in Oncology. J Natl Compr Canc Netw 2021;19:77-102.
28. Tomita N, Ishida H, Tanakaya K, et al. Japanese Society for Cancer of the Colon and Rectum (JSCCR) guidelines 2020 for the Clinical Practice of Hereditary Colorectal Cancer. Int J Clin Oncol 2021;26:1353-419.
29. Medical Administration Department of National Health Commission, Chinese Society of Clinical Oncology, Gu J, Wang J. Chinese protocol of diagnosis and treatment of colorectal cancer of the National Health Commission (2023 edition). J Digest Oncol 2023;15:177-206.
30. Ren Y, Zhang H, Tian J, et al. Comparison of clinical value of laparoscopic SMA and left-sided SMV D3 radical resection for right hemi-bowel cancer. Chin J Oper Proc Gen Surg 2021;15:104-6.
31. Nesgaard JM, Stimec BV, Ignjatovic D. Comments on Superior Mesenteric Artery First Approach for Right Colectomy. Ann Surg Oncol 2022;29:7923-4.
32. Zhou J, Chen J, Wang M, et al. A study on spinal level, length, and branch type of the inferior mesenteric artery and the position relationship between the inferior mesenteric artery, left colic artery, and inferior mesenteric vein. BMC Med Imaging 2022;22:38.
33. Murono K, Kawai K, Ishihara S, et al. Evaluation of the vascular anatomy of the right-sided colon using three-dimensional computed tomography angiography: a single-center study of 536 patients and a review of the literature. Int J Colorectal Dis 2016;31:1633-8.

34. Gamo E, Jiménez C, Pallares E, et al. The superior mesenteric artery and the variations of the colic patterns. A new anatomical and radiological classification of the colic arteries. Surg Radiol Anat 2016;38:519-27.
35. Balcerzak A, Tubbs RS, Waśniewska-Włodarczyk A, et al. Classification of the superior mesenteric artery. Clin Anat 2022;35:501-11.

Cite this article as: Chen J, Tian H, Yu K, Tao S, Bai B, Song A, Gu H. The clinical value of spectral computed tomography reconstruction technology for the anatomy of the superior mesenteric artery in laparoscopic radical right hemicolectomy for colon cancer: a cross-sectional study. J Gastrointest Oncol 2025;16(4):1461-1473. doi: 10.21037/jgo-2025-167